Geochemical Journal, Vol. 52, pp. 531 to 540, 2018 doi:10.2343/geochemj.2.0541

U-Pb dating of calcite using LA-ICP-MS: Instrumental setup for non-matrix-matched age dating and determination of analytical areas using elemental imaging

Tatsunori Yokoyama,[1]* Jun-ichi Kimura,[2]* Takehiro Mitsuguchi,[1] Toru Danhara,[3] Takafumi Hirata,[4] Shuhei Sakata,[5] Hideki Iwano,[3] Seiji Maruyama,[3] Qing Chang,[2] Takashi Miyazaki,[2] Hiroaki Murakami[1] and Yoko Saito-Kokubu[1]

[1]Tono Geoscience Center, Japan Atomic Energy Agency (JAEA), Jorinji, Izumicho, Toki 509-5102, Japan
[2]Department of Solid Earth Geochemistry, Japan Agency for Marine-Earth Science and Technology (JAMSTEC), 2-15 Natsushima-cho, Yokosuka 237-0061, Japan
[3]Kyoto Fission-Track Co., Ltd., Omiya, Kita-ku, Kyoto 603-8832, Japan
[4]Geochemistry Research Center, Graduate School of Science, The University of Tokyo, Hongo, Tokyo 113-0033, Japan
[5]Department of Chemistry, Gakushuin University, Mejiro 1-5-1, Toshima-ku, Tokyo 171-8588, Japan

(*Received March 5, 2018; Accepted September 19, 2018*)

We developed a non-matrix matched U-Pb dating method for calcite by using excimer laser ablation-multiple Faraday collector-inductively coupled plasma-mass spectrometry (LA-MFC-ICP-MS). The excimer LA was set to generate a low-aspect-ratio crater of 100 μm diameter × 50 μm depth to minimize downhole U-Pb fractionation. We used He sample ablation gas mixed with Ar carrier gas and additional trace N_2 gas to create a robust plasma setup in MFC-ICP-MS. The use of N_2 additional gas allowed for low oxide molecular yield ($UO^+/U^+ < 1\%$) for high-sensitivity JET-sampler and X-skimmer interface cones with the ICP shield electrode disconnected. Moreover, this resulted in robust ICP plasma against different matrixes in LA aerosols owing to efficient dissociation-ionization of the aerosols by increased plasma temperature. The above setup helped accomplish accurate U-Pb dating of calcite samples by using SRM 612 glass from the National Institute of Standards and Technology (NIST) as the standard. We applied this method to the following calcite samples: (1) recently-proposed reference material named WC-1 with a determined U-Pb age of 254.6 ± 3.2 Ma and (2) a well-preserved fossil specimen of blastoid *Pentremites* sp. with an estimated age of ~339–318 Ma. Prior to the U-Pb dating, quantitative two-dimensional maps of U, Th, and Pb isotope abundances of the calcite samples were obtained using a LA-ICP-MS imaging technique to select suitable areas for dating. Obtained U-Pb age of the WC-1 sample was 260.0 ± 6.7 Ma with an anchored point of initial $^{207}Pb/^{206}Pb$ ratio of 0.85 ± 0.02 determined by Roberts *et al*. (2017), which was close to the reported U-Pb age of 254.4 ± 0.8 Ma. The regression-based U-Pb discordant line age of the *Pentremites* sample was dated 332 ± 12 Ma, which indicate accurate U-Pb dating by this method.

Keywords: U-Pb dating, calcite, laser ablation ICP-MS, elemental imaging

Introduction

Calcite often precipitates from various types of geofluids. Therefore, U-Pb dating of calcite can provide unique information about the ages of fluids relevant to sediment diagenesis (Smith *et al*., 1991), ore formation (Brannon *et al*., 1996; Grandia *et al*., 2000), fault displacement (Roberts and Walker, 2016), evaporite formation (Becker *et al*., 2002), soil formation (Rasbury *et al*., 1997), and speleothem formation (Richards *et al*., 1998). Along with growing interest in U-Pb age dating of smaller calcite minerals or along the chemical zoning of a calcite mineral, U-Pb dating based on laser ablation inductively coupled plasma-mass spectrometry (LA-ICP-MS) has become a central analytical technique (Li *et al*., 2014; Roberts and Walker, 2016) compared to isotope dilution thermal ionization mass spectrometry (ID-TIMS) (Smith and Farquhar, 1989; Becker *et al*., 2002). However, there exist some difficulties in applying LA-ICP-MS U-Pb dating to calcite samples. Matrix-matched reference materials are prerequisites for U-Pb dating using LA-ICP-MS. The difficulty in U-Pb dating using LA-ICP-MS is associated with elemental fractionation between U and Pb during sample ablation at the LA site (Eggins *et al*., 1998; Horn and Blanckenburg, 2007; Ueda *et al*., 2018) and in the ICP plasma due to different matrixes of the samples and the reference materials (Kimura and Chang, 2012;

*Corresponding authors (e-mail: yokoyama.tatsunori@jaea.go.jp; jkimura@jamstec.go.jp)

Kroslakova and Günther, 2007). For zircon and monazite, which tend to yield concordant U-Pb ages, a few natural reference materials with concordant U-Pb ages have been proposed and used practically for U-Pb dating (Black *et al*., 2004; Cocherie *et al*., 2009; Kent, 2008; Kimura *et al*., 2011, 2013b; Paul *et al*., 2011). However, at present, initial calibration standards for the LA-ICP-MS U-Pb dating of calcite samples are yet to be available (yet to be synthesized). The apparent Pb/U distribution in calcite reference materials is usually heterogeneous, and it is difficult to simply estimate the elemental fractionation of Pb/U based on a comparison of the ratios between the measured and reference values of the reference material.

Because calcite contains initial Pb in its mineralogical lattice or boundaries of micro-calcite grains, U-Pb discordant line age is usually applied. This approach has often been employed in U-Pb dating with high common-Pb materials (e.g., Cox and Wilton, 2006; Simonetti *et al*., 2006; Chew *et al*., 2014). On the Tera-Wasserburg plot, initial $^{207}Pb/^{206}Pb$ is determined from an upper intercept of the vertical axis by the regression line through measured U-Pb data points. The $^{238}U/^{206}Pb$ age is then calculated from a lower intercept. A secondary calibration standard of U-bearing minerals, including calcite, has been proposed to correct for the elemental fractionation of ^{238}U and ^{206}Pb between samples and reference materials to access the age shifts (slope) of the U-Pb discordant lines (Iizuka *et al*., 2011; Chew *et al*., 2014; Li *et al*., 2014; Roberts *et al*., 2017). Recently, a natural calcite reference material with a discordant line U-Pb age of ~254 Ma has been proposed for LA-ICP-MS dating; this material can be used to correct the U-Pb discordant line of the calcite sample to accurately obtain the U-Pb age of the sample (Roberts *et al*., 2017).

In this paper, we carefully accessed the LA condition and ICP setups to minimize matrix-dependent variability in elemental fractionation between U and Pb, and accomplished accurate U-Pb age dating of calcite samples without using matrix-matched reference materials. The use of a 193-nm ultraviolet excimer LA system with low-aspect-ratio craters and He-ablation gas mixed with Ar-sample gas and N_2-additional gas by using high-efficiency sample-skimmer interface cones sufficiently minimized the matrix effect while keeping the instrumental sensitivity sufficiently high for MFC-ICP-MS (e.g., Hu *et al*., 2008; Fu *et al*., 2017). This allowed for the use of only a synthetic glass standard of the Standard Reference Material (SRM) 612 from the National Institute of Standards and Technology (NIST) for accurate U-Pb dating of calcite samples. Before the *in-situ* U-Pb dating of the calcite samples, we applied the LA-ICP-MS elemental imaging technique to the samples to obtain a distribution map of U, Th, and Pb isotopes, which were very useful to select suitable areas for dating.

Samples

We analyzed the following two samples: (1) calcite reference material (named WC-1) proposed for LA-ICP-MS U-Pb dating (Roberts *et al*., 2017) and (2) a well-preserved calcareous Carboniferous fossil specimen *Pentremites* sp. (an extinct genus of blastoid echinoderm). The WC-1 was collected from marine calcite cement obtained from a fault-related discordant Neptunian dike in the Permian (Capitanian) Reef Complex exposed in the Guadalupe Mountains on the western side of the Delaware Basin, New Mexico, USA. The U-Pb age of the WC-1 has been determined to be 254.6 ± 0.8 Ma (Roberts *et al*., 2017). The WC-1 sample used in this study was a rectangular slab (~7 mm × ~9 mm × ~2 mm; see Fig. 1a), which was given by Dr. Nick Roberts. The *Pentremites* specimen (~13–20 mm in diameter; see Fig. 1b) was collected from the strata of the Chesterian age (from mid-Mississippian to earliest Pennsylvanian) in northeastern Oklahoma, USA, corresponding to an estimated age of ~339 to ~318 Ma (Galloway and Kaska, 1957; Fabian, 1987). X-ray diffraction analyses of this specimen detected only calcite for the skeletal (calyx) part and calcite with a few or several % of quartz for the detrital infilling part (see Supplementary Fig. S1). It is known that almost all echinoderms, including extinct blastoids, secrete calcitic skeletons.

Methods and Analytical Settings

Elemental imaging technique

We applied the LA-ICP-MS elemental imaging technique to the WC-1 and *Pentremites* samples to obtain distribution maps of the U, Th, and Pb isotopes of each sample by using a Photon-Machines Analyte G2 excimer laser ablation system connected to an Agilent 7700 ICP-MS at Tono Geoscience Center, Japan Atomic Energy Agency (JAEA). This technique was very useful for selecting suitable areas for our LA-ICP-MS *in-situ* U-Pb dating (i.e., areas of higher ^{238}U concentration and higher $^{206}Pb/^{208}Pb$ ratio) (Suzuki *et al*., 2018). Instrumental settings of the imaging technique are given in Supplementary Table S1.

LA-MFC-ICP-MS setup for U-Pb dating

We used a 193-nm Excimer Laser Ablation (ExLA) system (OK-ExLA2000, OK Lab, Tokyo, Japan) at the Department of Solid Earth Geochemistry, Japan Agency for Marine-Earth Science and Technology (DSEG/JAMSTEC) (Kimura and Chang, 2012). The ExLA system employs an ultraviolet excimer laser source by COMPex-102 (Coherent, California, USA). An imaging objective lens array made of excimer laser-grade high-power fused silica was used to focus the beam on the sam-

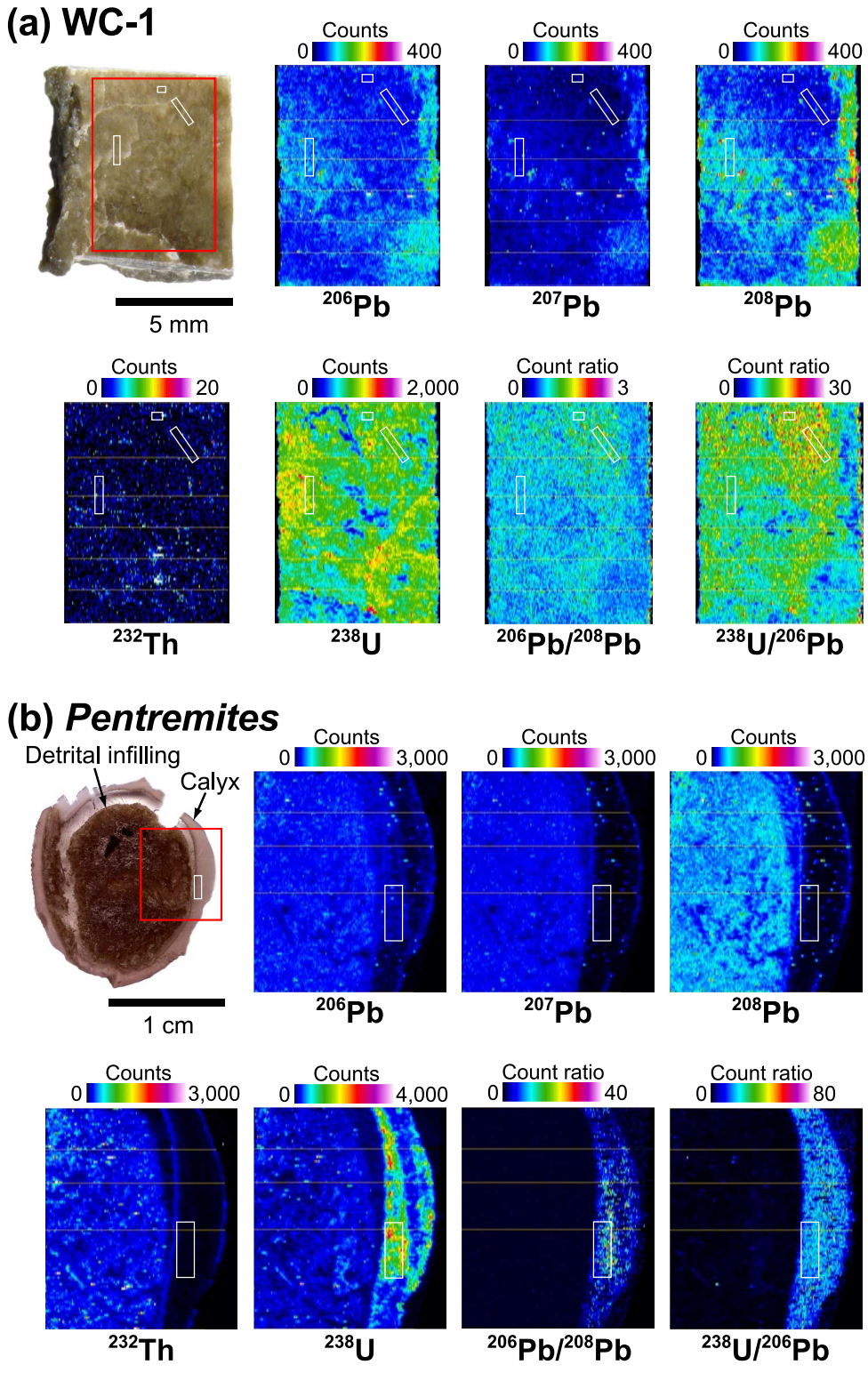

Fig. 1. Elemental imaging maps of (a) WC-1 and (b) Pentremites calcite samples analyzed using LA-ICP-QMS. Red squares indicate areas of elemental imaging. White boxes show analysis areas for U-Pb dating. See text for details.

Table 1. Instrumental setup of lasers and MFC-ICP-MS

Excimer laser	OK ExLA2000 (OK Lab)
Laser source	193 nm/20 ns ComPex102 (Coherent)
Pulse width	20 ns
Pulse energy	70 mJ
Focusing objective lens	Imaging optics using field lens and air spaced doublet objective
Beam diameter	100 μm diameter
Repetition rate	10 Hz
Laser fluence	~5 J cm^{-2} on sample surface
MFC-ICP-MS	Neptune (Thermo Scientific) modified
RF-power	1500 W
Guard electrode	Off (disconnected)
Sampling cone	JET-sample cone (Ni)
Skimmer cone	X-skimmer cone (Ni)
Cool gas (Ar)	13 L/min
Auxiliary gas (Ar)	1.0 L/min
Sample gas (Ar)	0.85 L/min
Laser carrier gas (He)	1.15 L/min
Laser add gas (N_2)	30 mL/min
Interface vacuum with E2M80	1.5 mbar with He ablation and N_2 add career gas
Mass resolution	Low resolution
Acquisition time	~0.5 s × 60 scans
Dispersion Quad	19.9 ($^{219.62}$M center mass with zoom optics)
Focus Quad	2
Cup and amplifier configurations	
^{204}Pb (^{204}Hg)	FC L4; 10^{11} Ω resistor amplifier
^{206}Pb	FC L3; 10^{12} Ω resistor amplifier
^{207}Pb	FC L2; 10^{12} Ω resistor amplifier
^{208}Pb	FC L1; 10^{11} Ω resistor amplifier
$^{219.62}$M	FC Axial; 10^{11} Ω resistor amplifier (not observed in data acquisition)
^{232}Th	FC H2; 10^{11} Ω resistor amplifier
^{238}U	FC H4; 10^{11} Ω resistor amplifier
Background subtraction	On-peak background; 30 s × 2

FC: Faraday cup; isobaric atomic and molecular ions are shown in parentheses.

ple surfaces. The resultant crater was set to have a diameter of 100 μm. The laser fluence on the sample surface was ~5 J cm^{-2} throughout the experiments. The resultant craters were ~50 μm deep after ablation for ~30 s with a laser repetition rate of 10 Hz (~0.17 μm per shot). For detailed descriptions of the instruments and settings, see Table 1.

Helium (1.15 L/min) was used as the ablation gas (Eggins *et al*., 1998; Horn and Günther, 2003). After the ablation cell, He gas was mixed with Ar sample gas (~0.85 L/min) in a cylindrical mixing chamber with an inner volume of 70 cm^3 (Kimura *et al*., 2012). The pulsed signals at low laser repetition rate were sufficiently smoothed out, and the washout time to the gas blank level by using this mixing device was about 20 s, which is sufficiently short for normal operation (Kimura *et al*., 2011, 2013a). Additional N_2 gas (30 mL/min) was then loaded into the mixed Ar-He sample gas just before the ICP torch. This additional gas was used to improve elemental sensitivity (Hu *et al*., 2008), but careful tuning with N_2 gas allowed for a low oxide molecular yield (Witte and Houk, 2012), which is important for non-matrix-matched measurement of stable isotopes (Fu *et al*., 2017) and for U-Pb dating of calcite samples (see below).

The ExLA system was coupled to a modified Neptune multiple-Faraday-collector (MFC)-ICP-MS (Thermo Fisher Scientific, Bremen, Germany) at DSEG/JAMSTEC. The MFC-ICP-MS interface was modified by the addition of a high-efficiency rotary pump for achieving a high transmission condition (Kimura *et al*., 2013a). The JET-sampler and X-skimmer cones were used and the guard electrode (GE) ICP shield was turned off to achieve the best instrument sensitivity with the lowest oxide yield, ~1500 V ppm^{-1} or ~94 Gcps ppm^{-1} Pb in solution mode using an Aridus II desolvating nebulizer and oxide yield of $^{238}U^{16}O^+/^{238}U^+ < 1\%$ in both the Aridus and the LA modes. This sensitivity is about a half of our previous application of LA-MFC-ICP-MS (JET-X comes

with GE on and no N_2 additional gas) to U-Pb dating, which used ~3000 V ppm^{-1} or 188 Gcps ppm^{-1} (Kimura *et al*., 2015).

The configuration of the Faraday collectors and Faraday amplifiers is given in Table 1, along with other instrumental settings. Two high-gain amplifiers using a 10^{12} Ω resistor (Koornneef *et al*., 2013) were assigned to the two target isotopes of ^{206}Pb and ^{207}Pb, whereas amplifiers using a 10^{11} Ω resistor were assigned to ^{232}Th, ^{238}U, and ^{204}Pb (Table 1). Gain calibration was performed daily by applying 3.33 V before any sample analysis. On-peak background baselines were measured twice for 30 s prior to signal acquisition in each analytical run. This measurement eliminated any cone memories and gas blanks, including ^{204}Hg interference on ^{204}Pb (Table 1) (Kimura *et al*., 2013b, 2015). The ^{204}Pb signal was not used in this study, but it was always monitored to detect any initial Pb in the analyzed spots. The observed ^{204}Pb signal intensities were 0.02–0.07 mV for the WC-1 sample and 0.09–0.38 mV for the *Pentremites* sample. The initial Pb may have originated from the calcite itself, contaminated Pb in cracks/grain boundaries, or Pb-bearing detrital grains.

Robust ICP-MS and LA setup

Oxide molecular yield under the highest sensitivity setup was very high at 30–50% (Kimura *et al*., 2015). Oxide yield decreased to ~1% by reducing sample gas flow, but this reduced instrument sensitivity by one tenth. This high oxide yield was a trade-off of the highest sensitivity setting needed for U-Pb dating using MFC-ICP-MS. Previous reports indicated that such the extreme settings should not be used to avoid matrix-dependent isotopic/elemental fractionation (Kimura *et al*., 2013a; Newman, 2011; Newman *et al*., 2009) and spectral interference of oxide ions (Kimura *et al*., 2013c). The sample-standard bracketing can accommodate U-Pb fractionation only when matrix-matched bracketing standard is used (Black *et al*., 2004; Cocherie *et al*., 2009; Kent, 2008; Kimura *et al*., 2011, 2013b; Paul *et al*., 2011).

The use of additional N_2 gas in the GE-off mode (see above and Table 1) allowed for low oxide yield while maintaining high sensitivity of ~1500 V/ppm against ~3000 V/ppm. This sensitivity along with the low oxide yield was a requisite for precise U-Pb dating of calcite samples using NIST SRM 612 glass as the initial calibration standard because no calcite reference material was available in which ^{206}Pb/^{238}U is homogeneously distributed and the ratio is accurately determined by other methods (e.g., ID-TIMS). PbO^+ was not observed in any instrumental setups, whereas the UO^+ yield was significant in our previous high-sensitivity setup (Kimura *et al*., 2015). UO^+ is formed more effectively than PbO^+ owing to the difference in oxide-dissociation energy, which is higher for U (=749 kJ mol^{-1}) relative to that for Pb (=397 kJ mol^{-1}) (Darwent, 1970). The oxide-dissociation of U ($^{238}U^{16}O^+/^{238}U^+ < 1\%$) was achieved by addition of N_2, perhaps owing to the increased plasma temperature behind the interface cones, which maintained the plasma in an energy state sufficiently high for UO^+ dissociation (Witte and Houk, 2012). Moreover, it has been reported that the use of both N_2 and He produced the lowest MO^+/M^+ signal ratio and the highest plasma gas temperature in the ICP and at the position sampled in the ICP owing to the combined effects of increased plasma temperature by N_2 and increased thermal conductivity by He in the plasma conduit (Witte and Houk, 2012).

Moreover, additional N_2 gas increased the viscosity of the sample plasma gas by allowing for the use of a lower Ar sample gas flow rate (0.85 L/min, see Table 1) than that of the Ar-He mixture (1.15 L/min see Kimura *et al*., 2015) by increasing the conductance of plasma gas at the interface cones. This was deduced from the vacuum pressure behind the JET-sampler cone (i.e., expansion chamber pressure), which was 1.5 mbar in this study (Table 1) as opposed to 1.8 mbar in case of the He-Ar mixture setup (see Kimura *et al*., 2015). The lower sample gas flow rate allowed for a longer transit time of LA aerosols in the ICP, thus assuring better, if not complete, dissociation-ionization (Fu *et al*., 2017). The combined effects of these phenomena helped form robust ICP plasma.

Non-matrix-matched measurement of calcite U-Pb ages was accomplished using novel setups of LA and MFC-ICP-MS. With these setups, U-Pb fractionation was negligible between the SRM 612 glass standard and the calcite samples. This was achieved by the combined use of the low-aspect-ratio LA crater, that prevented element fractionation due to preferential redeposition of the analytes onto the crater walls (100 μm diameter × 50 μm depth) (Horn and Blanckenburg, 2007), and the robust ICP operational setup. The former minimized downhole elemental fractionation, and the latter eliminated elemental fractionation in the ICP, both of which are matrix-dependent.

Data collection, reduction, and U-Pb age calculation

In this study, the WC-1 and *Pentremites* samples were used as unknowns for the novel matrix-independent U-Pb dating proposed herein. SRM 612 standard glass was used as the external standard. A standard and an unknown were analyzed, usually resulting in 15 unknowns and 16 standard data points, respectively, for one age dataset.

Each measurement consisted of two 30 s baseline measurements, followed by an idle time of 10 s with the laser on. Sixty acquisition cycles were recorded with ~0.5 time slices for 100 μm/10 Hz raster craters. The 10 s idle time assured stabilization of the 10^{12} Ω Faraday amplifiers (Horstwood *et al*., 2003; Kimura *et al*., 2013a, b). No

significant effect of the slow response time of the amplifiers (Hirata *et al.*, 2003) was observed with the hardware using a feedback circuit at the Faraday amplifier at the minimal response time (smallest Tau-factor setup) and with this protocol, partly owing to the use of a large sample gas mixing device. The baseline signals were subtracted from the total signals for each isotope peak. The net intensities (V) were used for isotope ratio calculations. Because standard bracketing was used and no matrix-dependence was observed, no further mass-bias correction was performed.

A dataset from each spot consisted of 30 isotope ratios of $^{206}Pb/^{238}U$ and $^{207}Pb/^{206}Pb$. In the case of high contribution of common Pb along clacks and the analysis of Pb-bearing detrital grains, fewer scans were used after TRA treatment by discarding scans with a high ^{208}Pb signal intensity. Monitoring of the ^{208}Pb signal was useful because of the low initial ^{232}Th in the calcite samples. An arithmetic mean and error of 1SD (1-standard deviation) were obtained for each run. The isotope ratios obtained in this way for the unknown from a single spot were then re-calculated using the reference isotope ratios of the standard by normalizing to two averaged sets of isotope ratios from the bracketing standard spots before and after the unknown. Error propagation between bracketing standards and bracketed unknowns were calculated with the 95% confidence limit (Kragten, 1994). We then obtained $^{207}Pb/^{235}U$, $^{206}Pb/^{238}U$, and $^{207}Pb/^{206}Pb$ ages of each single spot of the unknown with a weighted mean and error.

The error correlations between the isotope ratios, obtained using a common isotope, were calculated for $^{207}Pb/^{235}U$ and $^{206}Pb/^{238}U$ (Schmitz and Schoene, 2007), where ^{235}U was calculated using the measured ^{238}U using natural abundances of these isotopes (0.72/97.2745) (International_Union_of_Pure_and_Applied_Chemistry, 1984). Finally, discordant line U-Pb age (Faure, 1977) was calculated with all spot analyses data by using the Isoplot ver. 2.2 (Ludwig, 2001). The reference isotope ratios of SRM 612 were $^{207}Pb/^{206}Pb = 0.90745$ (Baker *et al.*, 2004) and $^{206}Pb/^{238}U = 0.2517$, which were calculated from the latest GeoReM (2017) reference values of Pb = 38.57 ppm and U = 37.38 ppm (Jochum *et al.*, 2005) and Pb isotope ratios (Baker *et al.*, 2004).

Results

Imaging of U, Th and Pb distribution

The imaging results of the WC-1 sample show considerable heterogeneity of ^{238}U and initial Pb (Fig. 1a), which is consistent with observations of Roberts *et al.* (2017). For LA-ICP-MS U-Pb dating of this sample, we selected areas where both ^{238}U and $^{206}Pb/^{208}Pb$ are relatively high (the two upper-right boxed areas in Fig. 1a)

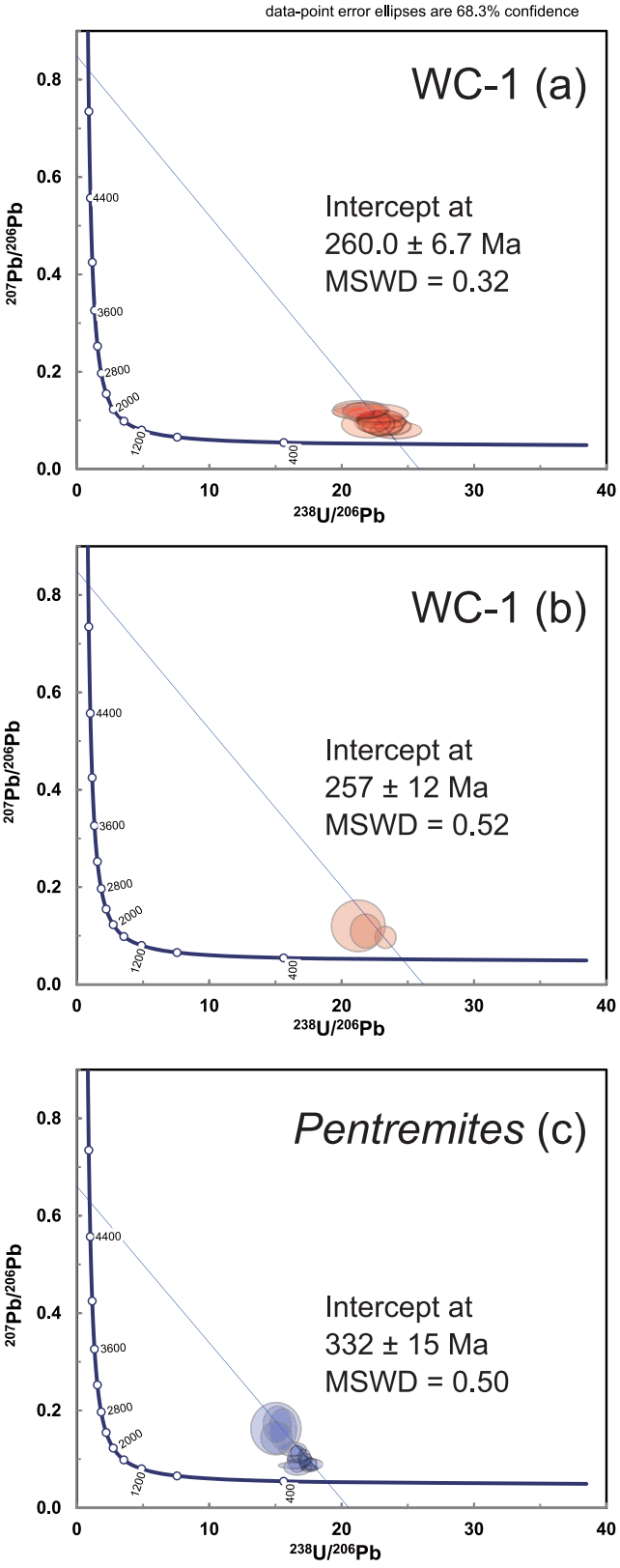

Fig. 2. U-Pb ages of WC-1 and Pentremites calcite samples determined by SRM 612 glass standard. (a) U-Pb discordant line age for WC-1, (b) WC-1 analyzed with (c) Pentremites in the same analytical session.

Table 2. U-Pb ages of the WC-1 and Pentremites calcite samples

Sample	U-Pb age (this study)	Reference age	Reference
WC-1 (LA-ICP-MS)	260.0 ± 6.7 Ma (n = 15) 257 ± 12 Ma (n = 3)*	254.4 ± 0.8 Ma (n = 214)	Roberts *et al.* (2017)
WC-1 (ID-TIMS)	not analyzed	254.4 ± 3.2 Ma (n = 10)	Roberts *et al.* (2017)
Pentremites sp. (LA-ICP-MS)	332.0 ± 15 Ma (n = 15)	339–318 Ma	Galloway and Kaska (1957), Fabian (1987)

All uncertainties of age are 1σ.
**Three spots in the WC-1 sample analyzed with the Pentremites sample (first-middle-last in the same run).*

and an area with relatively high ^{238}U and lower $^{206}Pb/^{208}Pb$ (the left boxed area in Fig. 1a) for comparison. The imaging results of the *Pentremites* sample indicate that the calyx part (consisting of the calcite phase only) contains areas where both ^{238}U and $^{206}Pb/^{208}Pb$ are very high and that no such areas exist in the detrital infilling part (consisting of calcite and a few or several % of quartz) (Fig. 1b). Most of the calyx part shows very low counts of ^{207}Pb and ^{208}Pb, and almost zero counts of ^{232}Th, whereas the detrital infilling part shows remarkably higher counts of these isotopes. The inner and outer boundaries of the calyx part indicate relatively higher counts of ^{206}Pb, ^{207}Pb, ^{208}Pb, and ^{232}Th, which is presumably due to adsorption of Pb and Th onto the calyx surface in marine and sedimentary environments. Within the calyx part, there are several tiny spots with remarkably higher counts of ^{206}Pb, ^{207}Pb, and ^{208}Pb but absence of ^{232}Th counts; on the other hand, the detrital infilling part shows significantly high counts of ^{206}Pb, ^{207}Pb, ^{208}Pb, and ^{232}Th, where these four isotopes show similar distributions. The Th/Pb inconsistency between the tiny spots and the detrital infilling suggests that the high-Pb spots within the calyx are not caused by particulate inclusions from the detrital infilling but due to some other type of contamination. These results suggest that at least the calyx areas with higher values of both ^{238}U and $^{206}Pb/^{208}Pb$ (typically in the white-line boxed area in Fig. 1b) are not or little affected by diagenetic contamination, and that the areas have remained an almost closed system concerning the U-Th-Pb systematics since the calyx formation in Chesterian seawater (~339–318 Ma) in the Mid-Carboniferous Period; thus, the white-line boxed area was selected for the LA-ICP-MS *in-situ* U-Pb dating. The $^{238}U/^{206}Pb$ variability in the calyx areas with higher ^{238}U and $^{206}Pb/^{208}Pb$ suggests variously discordant U-Pb ages.

U-Pb systematics

The analytical results of the WC-1 and *Pentremites* samples are shown in discordant lines normal Tera-Wasserburg plots in Fig. 2 and listed in Table 2. Individual datasets are given in Supplementary Table S2. The observed ^{204}Pb signal intensities were 0.02–0.07 mV for the WC-1 sample and 0.09–0.38 mV for the *Pentremites* sample. It is obvious that initial Pb was present in both of the samples. The Tera-Wasserburg discordant line plots were used with an anchored point of initial $^{207}Pb/^{206}Pb$ ratio of 0.85 ± 0.02 (Roberts *et al.*, 2017) for the WC-1 U-Pb age determination (Fig. 2). The obtained U-Pb age of the WC-1 sample was 260 ± 6.7 Ma (n = 15), which was very close to the previously-reported LA-ICP-MS U-Pb age of 254.4 ± 0.8 Ma and ID-TIMS age of 254.4 ± 3.2 Ma (Roberts *et al.*, 2017). This indicates that the age calibration of $^{238}U/^{206}Pb$ by using SRM 612 glass standard was matrix-independent. In fact, the discordant lines reproduced those reported by Roberts *et al.* (2017) (Fig. 2a and Table 2), indicating no $^{207}Pb/^{206}Pb$ and $^{238}U/^{206}Pb$ fractionation. It is worth noting that the secondary standard WC-1 is best suited for the test and yielded proper age without any additional correction. The U-Pb age of the *Pentremites* sample was dated 332 ± 15 Ma (n = 15) with an anchored point of initial $^{207}Pb/^{206}Pb$ ratio of 0.66 ± 0.14 (Fig. 2c and Table 2), corresponding almost to the center of the age range of this specimen (~339 to ~318 Ma).

Discussion and Conclusion

Calcite U-Pb dating is associated with two problems. One is the lack of a proper standard material with a similar matrix. The other is the presence of initial Pb, which results in a discordant line plot in U-Pb dating (see Fig. 2). The WC-1 is the first calcite that can provide discordant line, thus providing a correction factor in order to correct for the fractionation between U and Pb in U-Pb isotope analysis of calcite (Roberts *et al.*, 2017). This basically helps cope with the two aforementioned problems associated with U-Pb dating of calcite. A reproducibility test of the two isotope ratios showed proper U-Pb dating results of any unknowns, and thus, the WC-1 can be used as the secondary standard.

The resultant U-Pb age of the WC-1 sample determined by SRM 612 differed by 2.2% from the reference ID-TIMS age (Roberts *et al*., 2017) and was well within 1SD analytical error of 6.7 Ma, which is 2.6%. This matrix-independent analytical result is worth noting because of the significant reduction in statistical treatments for age correction of unknown samples. If any shifts were observed in the two isotope ratios measured using the WC-1, U-Pb ages of the measured unknowns should be force-corrected for the bias factors determined from the WC-1 measured in the same analytical session. In this case, error propagation should be considered from the viewpoint of analytical errors in $^{207}Pb/^{206}Pb$ and $^{206}Pb/^{238}U$ of both the secondary standard WC-1 and the initial standard (for example, SRM 612). If an unknown was measured without any mass/elemental fractionation, only the errors associated with the unknown measurements were effective without any effects of uncertainties in the secondary standard WC-1, even though error propagations from bracketing SRM 612 standards should have been considered as we did in our U-Pb dating. Moreover, the U-Pb age of the WC-1 sample measured in the same analytical session of the *Pentremites* sample was 257 ± 12 Ma (n = 3) (Fig. 2b and Table 2). This result further indicated the reproducibility of our analytical protocol. U-Pb age with less age bias was accomplished using the novel instrumental setups. In addition, elemental mapping obtained by LA-ICP-QMS prior to U-Pb dating was also useful to identify proper analytical areas for U-Pb ages.

We proposed novel instrumental setups and an analytical procedure that facilitates accurate and reproducible U-Pb age determination of calcite samples. Whether the same protocol can be applied to other U-bearing minerals (e.g., zircon or monazite) is a future research subject and will be explored and reported elsewhere.

Acknowledgments—Dr. Robert N. kindly provided the WC-1 sample to T.Y. The *Pentremites* specimen was provided by Nichika Inc. This project was carried out under a contract with METI as part of its R&D supporting program for developing geological disposal technology, and partly financially supported by JSPS KAKENHI JP15H02148 and JP16H01123 for J.-I.K. and A26247094 for T.H. Constructive comments from two anonymous reviewers improved and clarified the manuscript. We also thank to Dr. Y. Orihashi for editorial handling.

References

Baker, J., Peate, D., Waight, T. and Meyzen, C. (2004) Pb isotope analysis of standards and samples using a ^{207}Pb-^{204}Pb double spike and thallium to correct for mass bias with a double-focusing MC-ICP-MS. *Chem. Geol.* **211**, 275–303.

Becker, M. L., Rasbury, E. T., Meyers, W. J. and Hanson, G. N. (2002) U-Pb calcite age of the Late Permian Castile Formation, Delaware Basin: a constraint on the age of the Permian-Triassic boundary (?). *Earth Planet. Sci. Lett.* **203**, 681–689.

Black, L. P., Kamoc, S. L., Allen, C. M., Davis, D. W., Aleinikoff, J. N., Valleye, J. W., Mundilf, R., Campbell, I. H., Korsch, R. J., Williams, I. S. and Foudoulis, C. (2004) Improved $^{206}Pb/^{238}U$ microprobe geochronology by the monitoring of a trace-element-related matrix effect; SHRIMP, ID-TIMS, ELA-ICP-MS and oxygen isotope documentation for a series of zircon standards. *Chem. Geol.* **205**, 115–140.

Brannon, J. C., Cole, S. C., Podosek, F. A., Ragan, V. M., Coveney, R. M., Wallace, M. W. and Bradley, A. J. (1996) Th-Pb and U-Pb dating of ore-stage calcite and paleozoic fluid flow. *Science* **271**, 491–493.

Chew, D. M., Petrus, J. A. and Kamber, B. S. (2014) U-Pb LA-ICPMS dating using accessory mineral standards with variable common Pb. *Chem. Geol.* **363**, 185–199.

Cocherie, A., Fanning, C. M., Jezequel, P. and Robert, M. (2009) LA-MC-ICPMS and SHRIMP U-Pb dating of complex zircons from Quaternary tephras from the French Massif Central: Magma residence time and geochemical implications. *Geochim. Cosmochim. Acta* **73**, 1095–1108.

Cox, R. A. and Wilton, D. H. C. (2006) U-Pb dating of perovskite by LA-ICP-MS: An example from the Oka carbonatite, Quebec, Canada. *Chem. Geol.* **235**, 21–32.

Darwent, B. D. (1970) Bond dissociation energies in simple molecules. *National Standard Reference Series, National Bureau of Standards US* **NSRDS-NBS 31**, 1–48.

Eggins, S. M., Kinsley, L. P. J. and Shelley, J. M. G. (1998) Deposition and element fractionation processes during atmospheric pressure laser sampling for analysis by ICP-MS. *Appl. Surface Sci.* **127–129**, 278–286.

Fabian, R. (1987) Relation of biofacies to lithofacies in interpreting depositional environments in the Pitkin Limestone (Mississippian) in northeastern Oklahoma (Part I). *Shale Shaker* **37**, 76–95.

Faure, G. (1977) *Principles of Isotope Geology*. John Wiley & Sons, New York.

Fu, J., Hu, Z., Li, J., Yang, L., Zhang, W., Liu, Y., Li, Q., Zong, K. and Hu, S. (2017) Accurate determination of sulfur isotopes $\delta^{33}S$ and $\delta^{34}S$) in sulfides and elemental sulfur by femtosecond laser ablation MC-ICP-MS with non-matrix matched calibration. *J. Anal. Atom. Spectrom.* **32**, 2341–2351.

Galloway, J. J. and Kaska, H. V. (1957) Genus *Pentremites* and its species. *Geol. Soc. Am. Mem.* **69**, 1–114.

Grandia, F., Asmerom, Y., Getty, S., Cardellach, E. and Canals, À. (2000) U-Pb dating of MVT ore-stage calcite: implications for fluid flow in a Mesozoic extensional basin from Iberian Peninsula. *J. Geochem. Explor.* **69**, 377–380.

Hirata, T., Hayano, Y. and Ohno, T. (2003) Improvements in precision of isotopic ratio measurements using laser ablation-multiple collector-ICP-mass spectrometry: reduction of changes in measured isotopic ratios. *J. Anal. Atom. Spectrom.* **18**, 1283–1288.

Horn, I. and Blanckenburg, F. V. (2007) Investigation on elemental and isotopic fractionation during 196 nm femtosecond laser ablation multiple collector inductively coupled plasma mass spectrometry. *Spectrochim. Acta* **B62**, 410–422.

Horn, I. and Günther, D. (2003) The influence of ablation carrier gasses Ar, He and Ne on the particle size distribution and transport efficiencies of laser ablation-induced aerosols: implications for LA-ICP-MS. *Appl. Surface Sci.* **207**, 144–157.

Horstwood, M. S. A., Foster, G. L., Parrish, R. R., Noble, S. R. and Nowell, G. M. (2003) Common-Pb corrected *in situ* U-Pb accessory mineral geochronology by LA-MC-ICP-MS. *J. Anal. Atom. Spectrom.* **18**, 837–846.

Hu, Z., Gao, S., Liu, Y., Hu, S., Chen, H. and Yuan, H. (2008) Signal enhancement in laser ablation ICP-MS by addition of nitrogen in the central channel gas. *J. Anal. Atom. Spectrom.* **23**, 1093–1101.

Iizuka, T., Eggins, S. M., McCulloch, M. T., Kinsley, L. P. J. and Mortimer, G. E. (2011) Precise and accurate determination of $^{147}Sm/^{144}Nd$ and $^{143}Nd/^{144}Nd$ in monazite using laser ablation-MC-ICPMS. *Chem. Geol.* **282**, 45–57.

International_Union_of_Pure_and_Applied_Chemistry (1984) Element by element review of their atomic weights. *Pure Appl. Chem.* **56**, 695–768.

Jochum, K. P., Nohl, U., Herwig, K., Lammel, E., Stoll, B. and Hofmann, A. W. (2005) GeoReM: A new geochemical database for reference materials and isotopic standards. *Geostand. Geoanal. Res.* **29**, 333–338.

Kent, A. J. R. (2008) *In-situ* analysis of Pb isotope ratios using laser ablation MC-ICP-MS: Controls on precision and accuracy and comparison between Faraday cup and ion counting systems. *J. Anal. Atom. Spectrom.* **23**, 968–975.

Kimura, J.-I. and Chang, Q. (2012) Origin of the suppressed matrix effect for improved analytical performance in determination of major and trace elements in anhydrous silicate samples using 200 nm femtosecond laser ablation sector-field inductively coupled plasma mass spectrometry. *J. Anal. Atom. Spectrom.* **27**, 1549–1559.

Kimura, J.-I., Chang, Q. and Tani, K. (2011) Optimization of ablation protocol for 200 nm UV femtosecond laser in precise U-Pb age dating coupled to multi-collector ICP mass spectrometry. *Geochem. J.* **45**, 283–296.

Kimura, J.-I., Tani, K. and Chang, Q. (2012) Determination of Hf isotope ratios in zircon using multiple collector-inductively coupled plasma mass spectrometry equipped with laser ablation and desolvating nebulizer dual sample introduction system. *Geochem. J.* **46**, 1–12.

Kimura, J.-I., Chang, Q. and Kawabata, H. (2013a) Standardless determination of Nd isotope ratios in glasses and minerals using laser-ablation multiple-collector inductively coupled plasma mass spectrometry with a low-oxide molecular yield interface setup. *J. Anal. Atom. Spectrom.* **28**, 1522–1529.

Kimura, J.-I., Kawabata, H., Chang, Q., Miyazaki, T. and Hanyu, T. (2013b) Pb isotope analyses of silicate rocks and minerals with Faraday detectors using enhanced-sensitivity laser ablation-multiple collector-inductively coupled plasma mass spectrometry. *Geochem. J.* **47**, 369–384.

Kimura, J.-I., Takahashi, T. and Chang, Q. (2013c) A new analytical bias correction for *in situ* Sr isotope analysis of plagioclase crystals using laser-ablation multiple-collector inductively coupled plasma mass spectrometry. *J. Anal. Atom. Spectrom.* **28**, 945–957.

Kimura, J.-I., Chang, Q., Itano, K., Iizuka, T., Vaglarov, B. S. and Tani, K. (2015) An improved U-Pb age dating method for zircon and monazite using 200/266 nm femtosecond laser ablation and enhanced sensitivity multiple-Faraday collector inductively coupled plasma mass spectrometry. *J. Anal. Atom. Spectrom.* **30**, 494–505.

Koornneef, J. M., Bouman, C., Schwieters, J. B. and Davies, G. R. (2013) Use of 10^{12} ohm current amplifiers in Sr and Nd isotope analyses by TIMS for application to sub-nanogram samples. *J. Anal. Atom. Spectrom.* **28**, 749–754.

Kragten, J. (1994) Calculating standard deviations and confidence intervals with a universally applicable spreadsheet technique. *Analyst* **119**, 2161–2165.

Kroslakova, I. and Günther, D. (2007) Elemental fractionation in laser ablation-inductively coupled plasma-mass spectrometry: evidence for mass load induced matrix effects in the ICP during ablation of a silicate glass. *J. Anal. Atom. Spectrom.* **22**, 51–62.

Li, Q., Parrish, R. R., Horstwood, M. S. A. and McArthur, J. M. (2014) U-Pb dating of cements in Mesozoic ammonites. *Chem. Geol.* **376**, 76–83.

Ludwig, K. R. (2001) Isoplot v. 2.2—a geochronological toolkit for Microsoft Excel. Berkeley Geochronology Center, Special Publication, 1a, 53 pp.

Newman, K. (2011) Effects of the sampling interface in MC-ICP-MS: Relative elemental sensitivities and non-linear mass dependent fractionation of Nd isotopes. *J. Anal. Atom. Spectrom.* **27**, 63–70.

Newman, K., Freedman, P. A., Williams, J., Belshaw, N. S. and Halliday, A. N. (2009) High sensitivity skimmers and non-linear mass dependent fractionation in ICP-MS. *J. Anal. Atom. Spectrom.* **24**, 742–751.

Paul, B., Woodhead, J. D., Hergt, J., Danyushevsky, L., Kunihiro, T. and Nakamura, E. (2011) Melt inclusion Pb-isotope analysis by LA-MC-ICPMS: Assessment of analytical performance and application to OIB genesis. *Chem. Geol.* **289**, 210–223.

Rasbury, E. T., Hanson, G. N., Meyers, W. J. and Saller, A. H. (1997) Dating of the time of sedimentation using U-Pb ages for paleosol calcite. *Geochim. Cosmochim. Acta* **61**, 1525–1529.

Richards, D. A., Bottrell, S. H., Cliff, R. A., Ströhle, K. and Rowe, P. J. (1998) U-Pb dating of a speleothem of Quaternary age. *Geochim. Cosmochim. Acta* **62**, 3683–3688.

Roberts, N. M. W. and Walker, R. J. (2016) U-Pb geochronology of calcite-mineralized faults: Absolute timing of rift-related fault events on the northeast Atlantic margin. *Geology* **44**, 531–534.

Roberts, N. M. W., Rasbury, E. T., Parrish, R. R., Smith, C. J., Horstwood, M. S. A. and Condon, D. J. (2017) A calcite reference material for LA-ICP-MS U-Pb geochronology. *Geochem. Geophys. Geosyst.* **18**, 2807–2814.

Schmitz, M. D. and Schoene, B. (2007) Derivation of isotope ratios, errors, and error correlations for U-Pb geochronology using ^{205}Pb-^{235}U-(^{233}U)-spiked isotope dilution thermal ionization mass spectrometric data. *Geochem. Geophys. Geosyst.* **8**, doi:10.1029/2006GC001492.

Smith, P. E. and Farquhar, R. M. (1989) Direct dating of Phanerozoic sediments by the ^{238}U-^{206}Pb method. *Nature* **341**, 518–521.

Smith, P. E., Farquhar, R. M. and Hancock, R. G. (1991) Direct radiometric age determination of carbonate diagenesis using U-Pb in secondary calcite. *Earth Planet. Sci. Lett.* **105**, 474–491.

Simonetti, A., Heaman, L. M., Chacko, T. and Banerjee, N. R. (2006) In situ petrographic thin section U-Pb dating of zircon, monazite, and titanite using laser ablation-MC-ICPMS. *Int. J. Mass Spectrom.* **253**, 87–97.

Suzuki, T., Sakata, S., Makino, Y., Obayashi, H., Ohara, S., Hattori, K. and Hirata, T. (2018) iQuant2: Software for rapid and quantitative imaging using laser Ablation-ICP Mass Spectrometry. *Mass Spectrometry* **7**, A0065.

Ueda, H., Takazawa, E., Kato, R. and Adachi, Y. (2018) Evaluation of time-resolved mean-of-ratios reduction for laser ablation zircon U-Pb dating using quadrupole ICPMS. *Geochem. J.* **52**, 241–254.

Witte, T. M. and Houk, R. S. (2012) Origins of polyatomic ions in laser ablation-inductively coupled plasma-mass spectrometry: An examination of metal oxide ions and effects of nitrogen and helium in the aerosol gas flow. Spectrochim. *Acta Part B: Atomic Spectroscopy* **69**, 9–19.

Supplementary Materials

URL (http://www.terrapub.co.jp/journals/GJ/archives/data/52/MS541.pdf)
Figure S1
Tables S1 and S2